
Explainable Novel Category Discovery in Semantic Concept Space

Ifrat Ikhtear Uddin¹, Yang Zhou², KC Santosh¹, Longwei Wang^{1†},
ifratikhtear.uddin@coyotes.usd.edu, longwei.wang@usd.edu,
yangzhou@auburn.edu, kc.santosh@usd.edu

¹Department of Computer Science, University of South Dakota, USA

²Department of Computer Science and Software Engineering, Auburn University, USA

Abstract

Novel category discovery aims to identify unseen classes from unlabeled data by transferring knowledge from labeled categories, but most existing methods perform discovery in opaque latent feature spaces. As a result, they may separate novel categories accurately while providing little insight into what semantic evidence defines each discovered group. We propose **xNCD**, an explainable novel category discovery framework that performs both representation-based discovery and pseudo-label assignment directly in a structured semantic concept space. Instead of clustering arbitrary deep features, xNCD learns a label-free concept representation by aligning visual features with vision-language similarity priors from pretrained multimodal models, and then applies a unified labeled-and-unlabeled self-labeling objective over concept-space logits. This design makes each discovered category explainable by construction through stable concept signatures and instance-level concept evidence. Theoretically, we show that routing discovery through a semantic concept bottleneck induces a strict restriction of the feature-space hypothesis class, excluding a large family of unconstrained decision rules and biasing induced partitions toward semantically interpretable concept coordinates. Experiments on CIFAR-10, CIFAR-100, and CUB-200 demonstrate that xNCD preserves strong discovery performance while providing intrinsic explanations. Under task-agnostic evaluation, xNCD achieves 92.63% overall accuracy on CIFAR-10, close to UNO’s 93.4%, and improves CIFAR-100 overall accuracy from 73.2% to 76.45%, while being the only compared method that provides human-readable cluster- and instance-level explanations.

1 Introduction

Novel Category Discovery addresses the problem of identifying previously unseen semantic categories from unlabeled data while leveraging supervision from a set of known categories [1, 2]. This setting naturally arises in realistic deployments, where labeled data are limited to a subset of categories and new categories emerge over time. Recent advances in representation learning and clustering [3–18, 13, 19–25] have led to strong empirical performance on NCD benchmarks [26–28], demonstrating that high-quality embeddings can effectively separate known and novel categories.

Despite these successes, existing NCD methods largely operate in latent feature spaces whose dimensions lack explicit semantic meaning [29]. As a result, while novel categories may be correctly separated, the reason why a group of samples forms a distinct category remains opaque. This limitation makes it difficult to validate discovered categories, diagnose failure modes, or integrate

† Corresponding Authors.

human knowledge into the discovery process. Such opacity is particularly problematic in scientific, safety-critical, and human-in-the-loop applications [30–32], where interpretability and accountability are essential.

In this work, we argue that semantic interpretability should be an intrinsic property of the novel category discovery process, rather than a post hoc analysis applied after clustering. To this end, we propose an interpretable framework for NCD that performs representation learning and category discovery directly in a structured semantic concept space [33, 34]. Instead of relying on abstract embeddings, the framework learns a set of concept detectors whose activations form an explicit, human-readable intermediate representation for both labeled and unlabeled data.

A key challenge in adopting concept-based representations is the lack of concept annotations at scale [35]. To address this, we used a label-free concept projection learning strategy [36] that aligns learned concept activations with vision–language similarity priors derived from pretrained multimodal models [37]. This enables the framework to acquire semantically meaningful concept detectors without requiring manual concept supervision. Novel category discovery is then performed through a unified cross-entropy objective operating directly in concept space.

Experiments on CIFAR-10, CIFAR-100, and CUB-200 demonstrate competitive discovery performance while providing intrinsic, human-readable explanations for discovered categories. Our key contributions are:

- We introduce a novel category discovery framework that performs representation learning and category discovery directly in a structured semantic concept space. By mediating discovery through concept representations rather than latent embeddings, the framework produces novel categories that are intrinsically interpretable, with each category characterized by an explicit and human-readable concept signature.
- We formulate novel category discovery as a unified optimization problem over concept representations. Extensive experiments on CIFAR-10, CIFAR-100, and CUB-200 demonstrate competitive discovery performance while yielding stable and semantically meaningful explanations.
- We theoretically show that introducing a semantic concept bottleneck induces a strict restriction on the hypothesis space of novel category discovery models, eliminating semantically entangled feature-space decision rules and constraining the induced partitions of unlabeled data to be expressible through human-interpretable concept coordinates.

2 Related Works

Novel Category Discovery (NCD) addresses the problem of identifying unseen categories in unlabeled data while leveraging knowledge from labeled base categories. Early approaches KCL [38] and MCL [39] employed pairwise similarity learning but struggled with scalability. DTC [27] introduced deep transfer clustering, while RS+ [40] combined ranking statistics with pseudo-labeling. UNO [26] introduced a unified cross-entropy objective treating labeled and pseudo-labels homogeneously, with follow-up work extending NCD to generalized [41], open-world [42], and continual learning [1] settings. Despite strong clustering accuracy, all existing NCD methods operate in opaque feature spaces where discovered clusters carry no semantic meaning, preventing domain experts from validating discovered groupings.

While GCD [41] represents a more general formulation, our task-agnostic evaluation is directly comparable at test time, as both require joint classification without oracle task identity. The key distinction is in training: GCD mixes known samples into the unlabeled pool, while xNCD operates in the more controlled NCD setting where interpretability constraints are easier to enforce. Notably, GCD and subsequent methods [43] rely on ViT backbones pretrained with DINO on ImageNet, whereas xNCD uses ResNet-18/50 pretrained only on the labeled split.

Concept Bottleneck Models (CBMs) [33] introduce interpretability by routing predictions through human-understandable concept neurons, enabling transparent reasoning. Label-free CBM [36] removes the need for manual annotations by aligning concepts with vision-language priors. However, CBMs have been studied exclusively in closed-world settings with known categories. **This work is the first to extend concept bottleneck architectures to open-world learning**, performing discovery

in interpretable concept space rather than opaque features, and extending concept reasoning to scenarios where target categories are unknown.

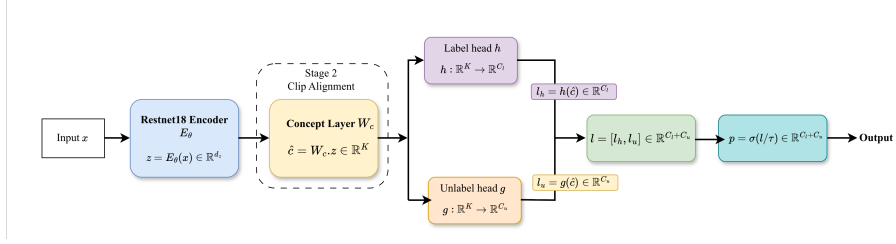


Figure 1: An input image x is processed by a pretrained encoder E_θ to produce features $z \in \mathbb{R}^{d_z}$. The concept projection layer W_c maps these features to interpretable concept activations $\hat{c} \in \mathbb{R}^K$, where each dimension corresponds to a human-understandable attribute. Two classification heads operate on concept activations: a labeled head h for known categories and an unlabeled head g for novel categories discovery. Logits are concatenated and passed through a unified softmax over all $C_l + C_u$ categories.

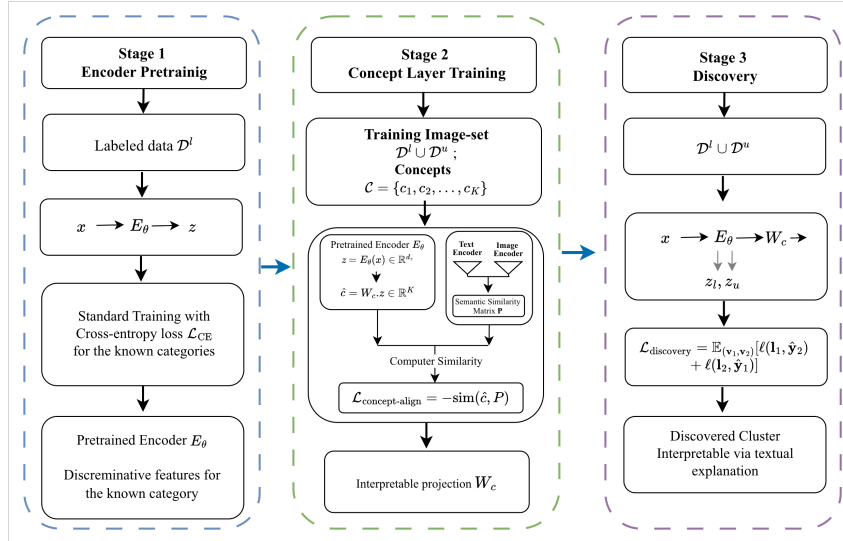


Figure 2: Overview of the xNCD framework. **Stage 1:** Encoder pretraining on labeled data with cross-entropy loss. **Stage 2:** Concept projection W_c is trained on all images by aligning concept activations with CLIP image-text similarities no concept annotations required. **Stage 3:** Novel categories are discovered by clustering in concept space, yielding interpretable clusters characterized by human-readable concept profiles (e.g., “four-legged, furry, wide mouth” for a dog cluster).

3 Methodology

3.1 Problem Formulation

In Novel Category Discovery (NCD), we are given a labeled dataset $\mathcal{D}^l = \{(\mathbf{x}_i^l, y_i^l)\}_{i=1}^{N_l}$ containing images from C_l known categories, and an unlabeled dataset $\mathcal{D}^u = \{\mathbf{x}_j^u\}_{j=1}^{N_u}$ containing images from C_u novel categories. The known and novel categories sets are disjoint. The goal is to discover and cluster the novel categories in \mathcal{D}^u by transferring knowledge learned from \mathcal{D}^l . Here we assume number of novel category is a known prior [26, 41, 44], as estimating number of novel category for NCD or GCD is considered a separate problem [45, 2].

Standard NCD methods discover clusters in high-dimensional feature spaces \mathbb{R}^{d_z} , producing opaque groupings that offer no insight into *why* samples belong together. We argue that interpretability and discovery are complementary: if we can represent images through human-understandable concepts,

we can both cluster effectively *and* explain what distinguishes each discovered category. To this end, we introduce **Explainable Novel Category Discovery (xNCD)**, which performs discovery in an interpretable concept space $\mathcal{C} = \{c_1, c_2, \dots, c_K\}$, where each c_j corresponds to a human-understandable visual attribute (e.g., “striped,” “four-legged,” “metallic”).

By representing images through K human-understandable concepts rather than d_z -dimensional latent features (where $K < d_z$), we constrain the hypothesis space to partitions expressible through interpretable semantic coordinates (formalized in Section 4). The key insight is that such concepts generalize across both known and novel categories: we can describe an unknown animal using attributes like “fur,” “tail,” and “four legs” without knowing its species name. This semantic grounding ensures that discovered clusters correspond to coherent conceptual groupings rather than arbitrary feature correlations.

3.2 Stage 1: Encoder Pretraining on Labeled categories

We pretrain a shared encoder $E_\theta : \mathbb{R}^d \rightarrow \mathbb{R}^{d_z}$ on the labeled dataset \mathcal{D}^l to learn discriminative features for known categories. The encoder outputs feature vectors $\mathbf{z} = E_\theta(\mathbf{x}) \in \mathbb{R}^{d_z}$, which are fed to a linear classifier $h : \mathbb{R}^{d_z} \rightarrow \mathbb{R}^{C_l}$ with C_l output neurons. The model is trained using standard cross-entropy loss:

$$\mathcal{L}_{\text{pretrain}} = -\frac{1}{N_l} \sum_{i=1}^{N_l} \sum_{c=1}^{C_l} \mathbf{y}_i^l[c] \log p_c^l(\mathbf{x}_i^l) \quad (1)$$

where $p^l = \sigma(h(E_\theta(\mathbf{x}))/\tau)$ is the softmax output with temperature τ , and \mathbf{y}^l is the one-hot encoded label.

3.3 Stage 2: Concept Layer Learning

The second stage learns to project encoder features into an interpretable concept space. The challenge is learning this projection *without* manual concept annotations for each image. We address this by leveraging CLIP as a concept supervisor.

CLIP as Concept Supervisor. For each image \mathbf{x}_i and concept c_j , we compute a target activation:

$$P_{ij} = E_{\text{CLIP}}^{\text{img}}(\mathbf{x}_i) \cdot E_{\text{CLIP}}^{\text{txt}}(c_j), \quad (2)$$

where $E_{\text{CLIP}}^{\text{img}}$ and $E_{\text{CLIP}}^{\text{txt}}$ are CLIP’s image and text encoders. The matrix $\mathbf{P} \in \mathbb{R}^{N \times K}$ provides dense supervision: P_{ij} is high when concept c_j is visually present in image \mathbf{x}_i .

Concept Projection Layer. We learn a projection matrix $\mathbf{W}_c \in \mathbb{R}^{K \times d_z}$ that maps encoder features to concept activations, following the label-free approach of Oikarinen et al. [36]:

$$\hat{\mathbf{c}} = \mathbf{W}_c E_\theta(\mathbf{x}) = \mathbf{W}_c \mathbf{z}, \quad (3)$$

where $\hat{\mathbf{c}} \in \mathbb{R}^K$ represents predicted concept activations. Each row of \mathbf{W}_c acts as a “concept detector” that identifies the corresponding visual attribute.

Training Objective. We train \mathbf{W}_c to align predicted concept activations with CLIP’s assessments. For concept j , let $\mathbf{q}_j = [\hat{c}_j(\mathbf{x}_1), \dots, \hat{c}_j(\mathbf{x}_N)]^\top \in \mathbb{R}^N$ be the activation pattern across all images. We maximize the similarity between \mathbf{q}_j and the corresponding column of the CLIP matrix $\mathbf{P}_{:,j}$ using a cubed cosine similarity:

$$\text{sim}(\mathbf{q}_j, \mathbf{P}_{:,j}) = \frac{\bar{\mathbf{q}}_j^3 \cdot \bar{\mathbf{P}}_{:,j}^3}{\|\bar{\mathbf{q}}_j^3\|_2 \|\bar{\mathbf{P}}_{:,j}^3\|_2}, \quad (4)$$

where $\bar{\mathbf{v}}$ denotes mean-centered and standardized \mathbf{v} , and the cube is applied element-wise. Standard cosine similarity weights all samples equally, but for concept alignment, we care most about images where the concept is clearly present. The cubing operation amplifies high-activation samples where CLIP confidently detects the concept, while suppressing noise from ambiguous cases, leading to sharper concept detectors, more details are in Appendix C.

The alignment loss over all concepts is:

$$\mathcal{L}_{\text{align}}(\mathbf{W}_c) = \sum_{j=1}^K -\text{sim}(\mathbf{q}_j, \mathbf{P}_{:,j}). \quad (5)$$

After training, we retain only concepts achieving $\text{sim}(\mathbf{q}_j, \mathbf{P}_{:,j}) > \delta_{\text{align}}$ on validation data, filtering out poorly-aligned concepts. We use $\delta_{\text{align}} = 0.35$ in our experiments. We also compute per-concept normalization statistics (μ_j, σ_j) for use in Stage 3.

3.4 Stage 3: Concept-based Discovery

The discovery stage performs unified learning on both labeled and unlabeled data, with all computations occurring in concept space rather than the original feature space. This is the key architectural modification that enables interpretability.

Architecture. Our architecture (Figure 1) routes all predictions through the concept bottleneck layer. Given an input image \mathbf{x} , we compute:

$$\mathbf{z} = E_{\theta}(\mathbf{x}) \in \mathbb{R}^{d_z}, \quad (6)$$

$$\tilde{\mathbf{c}} = \frac{\mathbf{W}_c \mathbf{z} - \boldsymbol{\mu}}{\boldsymbol{\sigma}} \in \mathbb{R}^K, \quad (7)$$

where $\boldsymbol{\mu}, \boldsymbol{\sigma} \in \mathbb{R}^K$ are per-concept normalization statistics from Stage 2. The normalized concept activations $\tilde{\mathbf{c}}$ are processed by two types of classification heads operating in concept space. A labeled head $h: \mathbb{R}^K \rightarrow \mathbb{R}^{C_l}$, implemented as a linear classifier, is responsible for predicting known categories. In parallel, a set of unlabeled heads $g_{n=1}^N$, each mapping $\mathbb{R}^K \rightarrow \mathbb{R}^{C_u}$ and implemented as an MLP-based clustering module, is used to discover novel categories.

We employ multiple clustering heads to prevent convergence to local optima during discovery. During training, for each batch, we iterate over clustering heads and compute logits by concatenating the labeled head with each clustering head independently:

$$\mathbf{l}_n = [h(\tilde{\mathbf{c}}), g_n(\tilde{\mathbf{c}})] \in \mathbb{R}^{C_l + C_u}, \quad n = 1, \dots, N. \quad (8)$$

The logits are passed through a shared softmax over all $C = C_l + C_u$ categories, enabling joint reasoning about known and novel categories. At test time, we use the head with lowest training loss in the final epoch.

Training Objective. We adopt multi-view self-labeling with swapped prediction [46, 26], where pseudo-labels from one augmented view supervise the other, encouraging transformation-invariant assignments. Crucially, all computations occur in concept space: pseudo-labels are computed from concept-space logits, ensuring that cluster assignments emerge from semantic concept similarities rather than opaque feature correlations.

The unified cross-entropy loss treats labeled supervision and pseudo-labels homogeneously:

$$\mathcal{L}_{\text{discovery}} = \mathbb{E}_{(\mathbf{v}_1, \mathbf{v}_2)} [\ell(\mathbf{l}_1, \hat{\mathbf{y}}_2) + \ell(\mathbf{l}_2, \hat{\mathbf{y}}_1)] \quad (9)$$

where $\mathbf{l}_1, \mathbf{l}_2$ are concept-space logits from views $\mathbf{v}_1, \mathbf{v}_2$, and $\hat{\mathbf{y}}_1, \hat{\mathbf{y}}_2$ are their swapped targets. Labeled targets are ground-truth labels padded with zeros; unlabeled pseudo-labels are generated via Sinkhorn-Knopp [47] applied to concept-space logits (see Appendix D). Each discovered cluster i is characterized by a semantic signature of its top- r activated and deactivated concepts ($r=5$); formal definitions are in Appendix E.

4 Concept Bottlenecks as Hypothesis Space Restriction for Novel Category Discovery

We formalize explainable novel category discovery as a problem of learning a classifier whose induced partition over unlabeled data is constrained to admit a meaningful semantic interpretation. Let $\mathcal{X} \subset \mathbb{R}^d$ denote the input space, and let $C = C_l + C_u$ be the total number of categories, consisting of C_l known categories with labels and C_u unknown (novel) categories to be discovered from unlabeled data. In this setting, a learned predictor implicitly defines a partition of the unlabeled dataset \mathcal{D}_u through its decision rule, typically via pseudo-labeling or clustering assignments.

Most existing novel category discovery (NCD) methods operate in a learned feature space and construct predictors of the form

$$f_{\text{feat}}(x) = \text{softmax}(W \phi_{\theta}(x)), \quad (10)$$

where $\phi_\theta : \mathcal{X} \rightarrow \mathbb{R}^{d_z}$ is a learned feature extractor (e.g., a deep convolutional encoder) and $W \in \mathbb{R}^{C \times d_z}$ is a linear classifier whose rows correspond to known and novel category logits. We denote the corresponding hypothesis class by

$$\mathcal{H}_{\text{feat}} = \{x \mapsto \text{softmax}(W \phi_\theta(x)) : \theta, W\}. \quad (11)$$

This hypothesis class is highly expressive, enabling strong empirical performance in separating known and unknown categories. However, its expressiveness also permits a vast family of decision boundaries and induced partitions that depend on arbitrary geometric correlations in feature space. As a result, clusters discovered under $\mathcal{H}_{\text{feat}}$ need not correspond to coherent or human-understandable semantic attributes, limiting interpretability and trust in open-world deployments.

Concept-Space Formulation. Our approach introduces an explicit semantic bottleneck that mediates all predictions through a structured concept space. Specifically, we define a concept map $c_\psi : \mathcal{X} \rightarrow \mathbb{R}^K$ with $K < d_z$, given by

$$c_\psi(x) = \tilde{c}(x) = \frac{W_c \phi_\theta(x) - \mu}{\sigma}, \quad (12)$$

where $W_c \in \mathbb{R}^{K \times d_z}$ is a learnable concept projection matrix, and (μ, σ) are per-concept normalization statistics estimated during concept training. Each coordinate of $c_\psi(x)$ corresponds to the activation of a human-understandable semantic concept (e.g., visual attributes or contextual properties).

Classification and novel category discovery are then performed entirely in concept space:

$$f_{\text{concept}}(x) = \text{softmax}(A c_\psi(x)), \quad (13)$$

where $A \in \mathbb{R}^{C \times K}$ aggregates both the labeled-category head and the novel-category discovery head(s). The resulting hypothesis class is

$$\mathcal{H}_{\text{concept}} = \{x \mapsto \text{softmax}(A c_\psi(x)) : \theta, \psi, A\}. \quad (14)$$

By construction, every prediction and pseudo-label assignment is a function of explicit concept activations, ensuring that the induced partition over \mathcal{D}_u is mediated by semantically interpretable coordinates.

Hypothesis Space Restriction. We now show that introducing a concept bottleneck does not merely reparameterize feature-space NCD, but instead induces a strict restriction on the underlying hypothesis space. This restriction eliminates a large family of decision rules that rely on arbitrary feature correlations and enforces that all predictions factor through a low-dimensional, semantically structured subspace.

Recall that feature-space NCD models admit predictors of the form

$$f_{\text{feat}}(x) = \text{softmax}(W \phi_\theta(x)),$$

where $W \in \mathbb{R}^{C \times d_z}$ is unconstrained. In contrast, concept-mediated models enforce a two-stage factorization

$$\phi_\theta(x) \longrightarrow c_\psi(x) \longrightarrow f_{\text{concept}}(x),$$

where all category logits are linear combinations of concept activations. We formalize this distinction below.

Proposition 4.1. *Assume $c_\psi(x)$ is linear in $\phi_\theta(x)$, i.e., $c_\psi(x) = W_c \phi_\theta(x)$ (ignoring normalization for clarity). Then*

$$\mathcal{H}_{\text{concept}} \subseteq \mathcal{H}_{\text{feat}}. \quad (15)$$

Moreover, if $K < \min\{C, d_z\}$, the inclusion is strict.

Proof. For any predictor $f_{\text{concept}} \in \mathcal{H}_{\text{concept}}$, the logits satisfy

$$A c_\psi(x) = A W_c \phi_\theta(x) = W' \phi_\theta(x),$$

where $W' = A W_c \in \mathbb{R}^{C \times d_z}$. Therefore, f_{concept} can be written as a feature-space classifier and belongs to $\mathcal{H}_{\text{feat}}$, establishing $\mathcal{H}_{\text{concept}} \subseteq \mathcal{H}_{\text{feat}}$.

However, W' is constrained to factor through the K -dimensional concept space. In particular, $\text{rank}(W') \leq K$, since it is the product of a $C \times K$ matrix and a $K \times d_z$ matrix. When $K < \min\{C, d_z\}$, there exist weight matrices in $\mathbb{R}^{C \times d_z}$ whose rank exceeds K and which therefore cannot be expressed in this factorized form. Consequently, these classifiers are excluded from $\mathcal{H}_{\text{concept}}$, implying strict containment. \square

Beyond dimensional restriction, our framework further constrains $\mathcal{H}_{\text{concept}}$ by enforcing alignment between concept activations and vision-language similarity priors during training. This alignment restricts the admissible concept maps c_ψ to a semantically anchored subset, preventing arbitrary rotations or drift of the bottleneck that could otherwise occur under unsupervised discovery objectives.

Remark 4.2. When $K < \min\{C, d_z\}$, the rank constraint eliminates all $W' \in \mathbb{R}^{C \times d_z}$ with $\text{rank}(W') > K$, strictly reducing the hypothesis class. In our experimental settings $K > C$ for all datasets (CIFAR-10: $K=131, C=10$; CIFAR-100: $K=422, C=100$; CUB-200: $K=453, C=200$), so $\text{rank}(W') \leq C < K$ holds trivially and the rank argument provides no additional restriction. CLIP alignment then constitutes the sole operative interpretability guarantee, constraining admissible concept maps to a semantically anchored subset of $\mathbb{R}^{K \times d_z}$ independently of the K -vs- C relationship.

Table 6 (Appendix H) provides empirical evidence of this trade-off: reducing concept vocabulary size K degrades clustering accuracy, confirming that hypothesis space restriction and discovery performance are directly coupled.

5 Experiments and Results

5.1 Experimental Setup

We evaluate xNCD on CIFAR-10, CIFAR-100 [48], and CUB-200 [49], split into disjoint labeled and unlabeled sets following standard NCD protocols (5+5, 80+20, and 170+30 respectively). We use ResNet-18 for CIFAR-10/100 and ResNet-50 for CUB-200; full training details are in Appendix F. We report labeled accuracy, novel category clustering accuracy via Hungarian matching [50], overall accuracy, NMI, and ARI, under both task-aware and task-agnostic protocols. The task-agnostic setting, which jointly discriminates over all $C_l + C_u$ categories without oracle task identity, is directly comparable to the GCD evaluation protocol [41]. Dataset statistics and concept generation details are in Appendix G and A.

5.2 Clustering Performance

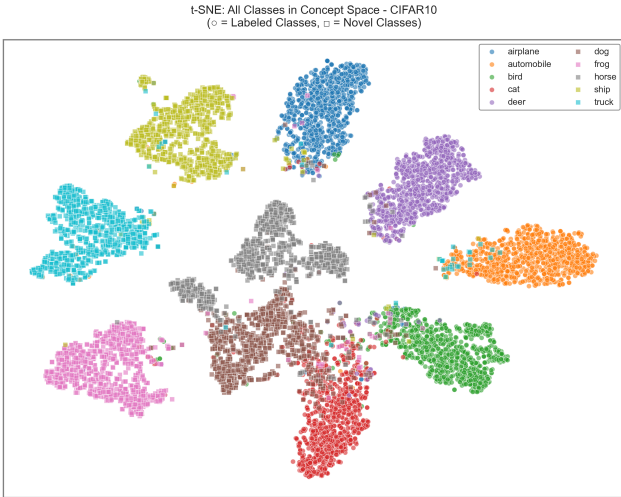


Figure 3: t-SNE visualization of concept space on CIFAR-10. Clear separation between all 10 categories (5 labeled, 5 novel) demonstrates that concept space preserves discriminative structure. Semantically similar categories (e.g., dog/cat, ship/airplane) cluster near each other.

Table 1 presents the quantitative results of xNCD across three benchmarks under both evaluation protocols.

CIFAR-10. xNCD achieves 95.28% overall under task-aware and 92.63% under task-agnostic evaluation (Table 1). The modest drop between protocols indicates effective separation of known from novel categories. Figure 3 shows clear concept-space separation across all 10 categories, with semantically similar categories (e.g., dog/cat, ship/airplane) clustering near each other.

Table 1: Clustering performance on CIFAR-10, CIFAR-100, and CUB-200 following the split mentioned in Table 3.

Dataset	Evaluation	Lab (%)	Unlab (%)	All (%)
CIFAR-10	Task-aware	97.46±0.2	93.10±0.4	95.28±0.3
	Task-agnostic	94.36±0.3	90.90±0.5	92.63±0.4
CIFAR-100	Task-aware	79.25±0.5	84.10±0.7	80.22±0.5
	Task-agnostic	76.78±0.4	75.15±0.6	76.45±0.5
CUB-200	Task-aware	70.88±0.3	50.85±0.6	67.88±0.4
	Task-agnostic	68.30±0.4	50.28±0.7	65.59±0.5

CIFAR-100. xNCD achieves 80.22% overall (task-aware) and 76.45% (task-agnostic). Notably, novel class accuracy (84.10%) exceeds labeled accuracy (79.25%) under task-aware evaluation, suggesting the concept bottleneck provides strong inductive bias for semantically coherent clustering.

CUB-200. xNCD achieves 67.88% overall (task-aware) and 65.59% (task-agnostic). The lower novel category accuracy (50.85%) reflects the challenge of fine-grained distinction, where subtle visual differences may not be fully captured by a general concept vocabulary.

We also evaluate clustering quality using NMI and ARI metrics. xNCD achieves NMI of 86.34% and ARI of 85.11% on CIFAR-10, indicating semantically coherent clusters. Detailed ablation studies on concept vocabulary size and clustering metrics are provided in Appendix H.

5.3 Comparison with State-of-the-Art

Table 2: Comparison with state-of-the-art methods on CIFAR-10 and CIFAR-100 using task-agnostic evaluation. We report accuracy on labeled categories (Lab), clustering accuracy on novel categories (Unlab), and overall accuracy (All). xNCD is the only method providing human-interpretable explanations for discovered clusters.

Method	CIFAR-10			CIFAR-100			Interpretable
	Lab	Unlab	All	Lab	Unlab	All	
KCL [38]	79.4	60.1	69.8	23.4	29.4	24.6	✗
MCL [39]	81.4	64.8	73.1	18.2	18.0	18.2	✗
DTC [27]	58.7	78.6	68.7	47.6	49.1	47.9	✗
RS+ [40]	90.6	88.8	89.7	71.2	56.8	68.3	✗
UNO [26]	93.5	93.3	93.4	73.2	73.1	73.2	✗
SNCD [28]	95.8	92.7	94.3	79.9	79.2	79.5	✗
GCD [41]	97.9	88.5	91.5	76.2	66.5	73.0	✗
xNCD (Ours)	94.36	90.90	92.63	76.78	75.15	76.45	✓

Table 2 compares xNCD against KCL [38], MCL [39], DTC [27], RS+ [40], UNO [26], SNCD [28], and GCD [41] under task-agnostic evaluation. On CIFAR-10, xNCD achieves 92.63% overall accuracy, competitive with UNO (93.4%) and GCD (91.5%), trailing SNCD (94.3%) by 1.67%. On CIFAR-100, xNCD outperforms UNO (73.2%) and GCD (73.0%) by over 3 points, remaining competitive with SNCD (79.5%). Critically, xNCD is the only compared method providing human-interpretable cluster- and instance-level explanations a capability that no accuracy metric can capture, yet is essential for validating discovered categories in scientific and safety-critical applications. The modest accuracy gap relative to non-interpretable methods confirms that routing discovery through a concept bottleneck does not significantly compromise clustering quality. Extended discussion is in Appendix I.

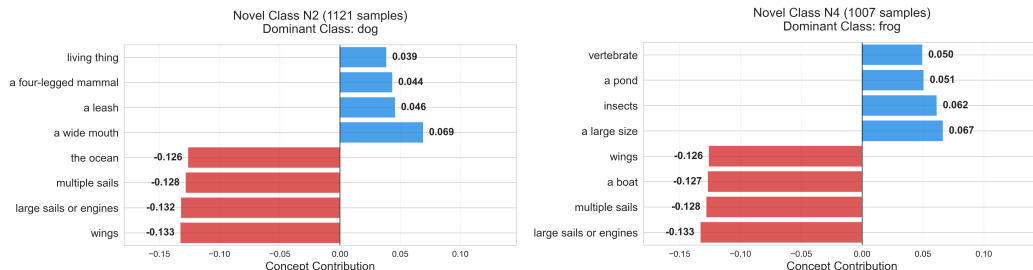


Figure 4: Concept activation profiles for discovered novel categories on CIFAR-10. The dog cluster (left) activates *living thing*, *four-legged mammal*, *wide mouth* while deactivating *ocean*, *wings*, correctly distinguishing terrestrial mammals from vehicles and birds. The frog cluster (right) activates *vertebrate*, *pond* while deactivating boat-related concepts.

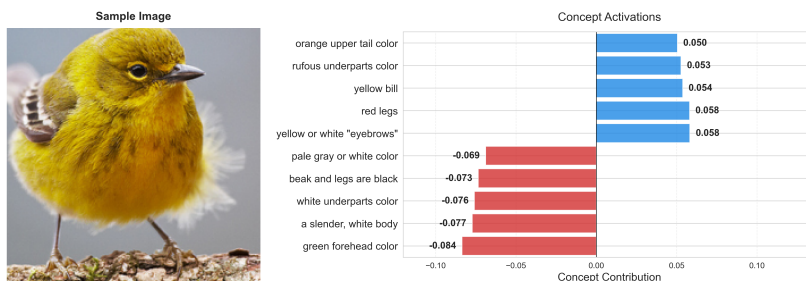


Figure 5: Instance-level concept attribution for a CUB-200 bird image. Activated concepts (blue) such as *yellow bill* and *yellow eyeball* provide positive evidence, while suppressed concepts (red) such as *green forehead* and *pale gray color* indicate absent attributes. Such explanations enable domain experts to validate discovered categories by understanding not just *what* the model predicts but *why*.

5.4 Interpretability Analysis

Cluster-Level Concept Signatures. Figure 4 visualizes concept profiles for discovered CIFAR-10 clusters. The dog cluster is characterized by strong positive activations for *living thing*, *four-legged mammal*, *wide mouth* while strongly deactivating *ocean*, *wings*, *sails*. These semantic signatures are highly informative: positive activations describe what the cluster *is*, while negative activations clarify what it is *not*. The dog cluster’s deactivation of ocean and wing concepts confirms the model correctly distinguishes terrestrial mammals from vehicles and birds.

Instance-Level Explanations. Figure 5 shows explanations for a CUB-200 bird image. The model highlights *yellow bill*, *rufous underparts*, *orange upper tail* as positive evidence while suppressing *green forehead*, *white underparts*. These instance-level explanations enable practitioners to understand not only *what* the model predicts but *why* a capability critical for deploying NCD in scientific domains where discovered categories must be validated by domain experts. Additional visualizations are in Appendix J.

6 Conclusion

We presented Explainable Novel Category Discovery (xNCD), a framework that performs novel category discovery directly in a semantic concept space, replacing opaque feature-space clustering with intrinsically interpretable discovery. By routing all predictions and pseudo-labels through a concept bottleneck learned via label-free alignment with vision–language priors, xNCD produces novel categories that admit concise, human-understandable concept signatures. We provide a theoretical analysis showing that concept bottlenecks impose a strict restriction on the hypothesis space of discovery models, eliminating semantically entangled partitions while preserving expressive power. Empirical results on CIFAR-10, CIFAR-100, and CUB-200 demonstrate that xNCD achieves competitive or improved discovery performance relative to state-of-the-art methods, while uniquely enabling transparent cluster- and instance-level explanations.

References

- [1] KJ Joseph, Sujoy Paul, Gaurav Aggarwal, Soma Biswas, Piyush Rai, Kai Han, and Vineeth N Balasubramanian. Novel class discovery without forgetting. In *European Conference on Computer Vision*, pages 570–586. Springer, 2022.
- [2] Kai Han, Sylvestre-Alvise Rebuffi, Sebastien Ehrhardt, Andrea Vedaldi, and Andrew Zisserman. Autonovel: Automatically discovering and learning novel visual categories. *IEEE Transactions on Pattern Analysis and Machine Intelligence*, 44(10):6767–6781, 2021.
- [3] Longwei Wang and Qilian Liang. Representation learning and nature encoded fusion for heterogeneous sensor networks. *IEEE Access*, 7:39227–39235, 2019.
- [4] Longwei Wang, Wen Chen, and Jun Li. Congestion aware dynamic user association in heterogeneous cellular network: A stochastic decision approach. In *2014 IEEE International Conference on Communications (ICC)*, pages 2636–2640. IEEE, 2014.
- [5] Longwei Wang, Chengfei Wang, Yupeng Li, and Rui Wang. Explaining the behavior of neuron activations in deep neural networks. *Ad Hoc Networks*, 111:102346, 2021.
- [6] Longwei Wang, Xianfu Chen, Zhifeng Zhao, and Honggang Zhang. Exploration vs exploitation for distributed channel access in cognitive radio networks: A multi-user case study. In *2011 11th International Symposium on Communications & Information Technologies (ISCIT)*, pages 360–365. IEEE, 2011.
- [7] Minyan Shi, Rui Wang, Erwu Liu, Zhixin Xu, and Longwei Wang. Deep reinforcement learning based computation offloading for mobility-aware edge computing. In *International conference on communications and networking in china*, pages 53–65. Springer International Publishing Cham, 2019.
- [8] Longwei Wang, Chengfei Wang, Yupeng Li, and Rui Wang. Improving robustness of deep neural networks via large-difference transformation. *Neurocomputing*, 450:411–419, 2021.
- [9] Kenan Xiao, Longwei Wang, Ashish Gupta, and Xiao Qin. Looking beyond content: Modeling and detection of fake news from a social context perspective. In *Proceedings of the 55th Hawaii International Conference on System Sciences 2022*, pages 1–10, 2022.
- [10] Longwei Wang, Peijie Chen, Chengfei Wang, and Rui Wang. Layer-wise entropy analysis and visualization of neurons activation. In *International Conference on Communications and Networking in China*, pages 29–36. Springer International Publishing Cham, 2019.
- [11] Longwei Wang, Xueqian Li, and Zheng Zhang. Dense cross-connected ensemble convolutional neural networks for enhanced model robustness. *arXiv preprint arXiv:2412.07022*, 2024.
- [12] Navid Nayyem, Abdullah Rakin, and Longwei Wang. Bridging interpretability and robustness using lime-guided model refinement. *arXiv preprint arXiv:2412.18952*, 2024.
- [13] Longwei Wang, Ifrat Ikhtear Uddin, Xiao Qin, Yang Zhou, and KC Santosh. Explainability-driven defense: grad-cam-guided model refinement against adversarial threats. In *Proceedings of the AAAI Symposium Series (AAAI) 2025*, volume 6, pages 49–57, 2025.
- [14] Robin Narsingh Ranabhat, Longwei Wang, Xiao Qin, Yang Zhou, and KC Santosh. Multi-scale unrectified push-pull with channel attention for enhanced corruption robustness. In *Proceedings of the AAAI Symposium Series 2025*, volume 6, pages 34–41, 2025.
- [15] Ifrat Ikhtear Uddin, Longwei Wang, and KC Santosh. Expert-guided explainable few-shot learning for medical image diagnosis. In *MICCAI Workshop on Data Engineering in Medical Imaging 2025*, pages 95–104. Springer Nature Switzerland, 2025.
- [16] Nicholas R Rasmussen, Rodrigue Rizk, Longwei Wang, and KC Santosh. Ecologically valid benchmarking and adaptive attention: Scalable marine bioacoustic monitoring. *arXiv preprint arXiv:2509.04682*, 2025.

- [17] KC Santosh, Rodrigue Rizk, and Longwei Wang. Toward carbon-neutral human ai: Rethinking data, computation, and learning paradigms for sustainable intelligence. In *2025 IEEE 7th International Conference on Cognitive Machine Intelligence (CogMI)*, 2025.
- [18] Longwei Wang, Ifrat Ikhtear Uddin, and KC Santosh. Expert-guided explainable few-shot learning with active sample selection for medical image analysis. *IEEE Journal of Biomedical and Health Informatics*, 2026.
- [19] Chaowei Zhang, Xiansheng Luo, Zewei Zhang, Yi Zhu, Jipeng Qiang, and Longwei Wang. Acting flatterers via llms sycophancy: Combating clickbait with llms opposing-stance reasoning. In *Proceedings of the ACM Web Conference (WWW) 2026*, pages 3195–3206, 2026.
- [20] Longwei Wang, Ifrat Ikhtear Uddin, Chaowei Zhang, Xiao Qin, and Yang Zhou. Bridging symmetry and robustness: On the role of equivariance in enhancing adversarial robustness. *Advances in Neural Information Processing Systems (NeurIPS)*, 38:159102–159129, 2025.
- [21] Nicholas R Rasmussen, Rodrigue Rizk, Longwei Wang, Arun Singh, and KC Santosh. Channel-selected stratified nested cross-validation for clinically relevant eeg-based parkinson’s disease detection. In *2026 IEEE Conference on Artificial Intelligence (CAI)*, pages 91–97. IEEE, 2026.
- [22] Casey Wall, Longwei Wang, Rodrigue Rizk, and KC Santosh. Winsor-cam: Human-tunable visual explanations from deep networks via layer-wise winsorization. *IEEE Transactions on Pattern Analysis and Machine Intelligence*, 2026.
- [23] Robin Narsingh Ranabhat, Longwei Wang, Amit Kumar Patel, and KC Santosh. Promoting shape bias in cnns: Frequency-based and contrastive regularization for corruption robustness. In *International Conference on Intelligent Systems and Pattern Recognition*, pages 16–26. Springer, 2025.
- [24] Puskal Khadka, Rodrigue Rizk, Longwei Wang, and KC Santosh. Coswin: Convolution enhanced hierarchical shifted window attention for small-scale vision. *arXiv preprint arXiv:2509.08959*, 2025.
- [25] Longwei Wang, Mohammad Navid Nayyem, Abdullah Al Rakin, KC Santosh, Chaowei Zhang, and Yang Zhou. Explainability-guided defense: Attribution-aware model refinement against adversarial data attacks. In *2025 IEEE International Conference on Data Mining (ICDM)*, pages 1585–1592. IEEE, 2025.
- [26] Enrico Fini, Enver Sanginetto, Stéphane Lathuilière, Zhun Zhong, Moin Nabi, and Elisa Ricci. A unified objective for novel class discovery. In *Proceedings of the IEEE/CVF international conference on computer vision*, pages 9284–9292, 2021.
- [27] Kai Han, Andrea Vedaldi, and Andrew Zisserman. Learning to discover novel visual categories via deep transfer clustering. In *Proceedings of the IEEE/CVF international conference on computer vision*, pages 8401–8409, 2019.
- [28] Weishuai Wang, Ting Lei, Qingchao Chen, and Yang Liu. Semantic-guided novel category discovery. In *Proceedings of the AAAI Conference on Artificial Intelligence*, volume 38, pages 5607–5614, 2024.
- [29] Wojciech Samek, Grégoire Montavon, Sebastian Lapuschkin, Christopher J Anders, and Klaus-Robert Müller. Explaining deep neural networks and beyond: A review of methods and applications. *Proceedings of the IEEE*, 109(3):247–278, 2021.
- [30] Cynthia Rudin. Stop explaining black box machine learning models for high stakes decisions and use interpretable models instead. *Nature machine intelligence*, 1(5):206–215, 2019.
- [31] Zachary C Lipton. The mythos of model interpretability: In machine learning, the concept of interpretability is both important and slippery. *Queue*, 16(3):31–57, 2018.
- [32] Finale Doshi-Velez and Been Kim. Towards a rigorous science of interpretable machine learning. *arXiv preprint arXiv:1702.08608*, 2017.

- [33] Pang Wei Koh, Thao Nguyen, Yew Siang Tang, Stephen Mussmann, Emma Pierson, Been Kim, and Percy Liang. Concept bottleneck models. In *International conference on machine learning*, pages 5338–5348. PMLR, 2020.
- [34] Mert Yuksekgonul, Maggie Wang, and James Zou. Post-hoc concept bottleneck models. *arXiv preprint arXiv:2205.15480*, 2022.
- [35] Been Kim, Martin Wattenberg, Justin Gilmer, Carrie Cai, James Wexler, Fernanda Viegas, et al. Interpretability beyond feature attribution: Quantitative testing with concept activation vectors (tcav). In *International conference on machine learning*, pages 2668–2677. PMLR, 2018.
- [36] Tuomas Oikarinen, Subhro Das, Lam M Nguyen, and Tsui-Wei Weng. Label-free concept bottleneck models. *arXiv preprint arXiv:2304.06129*, 2023.
- [37] Alec Radford, Jong Wook Kim, Chris Hallacy, Aditya Ramesh, Gabriel Goh, Sandhini Agarwal, Girish Sastry, Amanda Askell, Pamela Mishkin, Jack Clark, et al. Learning transferable visual models from natural language supervision. In *International conference on machine learning*, pages 8748–8763. PmLR, 2021.
- [38] Yen-Chang Hsu, Zhaoyang Lv, and Zsolt Kira. Learning to cluster in order to transfer across domains and tasks. *arXiv preprint arXiv:1711.10125*, 2017.
- [39] Yen-Chang Hsu, Zhaoyang Lv, Joel Schlosser, Phillip Odom, and Zsolt Kira. Multi-class classification without multi-class labels. *arXiv preprint arXiv:1901.00544*, 2019.
- [40] Kai Han, Sylvestre-Alvise Rebuffi, Sebastien Ehrhardt, Andrea Vedaldi, and Andrew Zisserman. Automatically discovering and learning new visual categories with ranking statistics. *arXiv preprint arXiv:2002.05714*, 2020.
- [41] Sagar Vaze, Kai Han, Andrea Vedaldi, and Andrew Zisserman. Generalized category discovery. In *Proceedings of the IEEE/CVF conference on computer vision and pattern recognition*, pages 7492–7501, 2022.
- [42] Kaidi Cao, Maria Brbic, and Jure Leskovec. Open-world semi-supervised learning. *arXiv preprint arXiv:2102.03526*, 2021.
- [43] Xin Wen, Bingchen Zhao, and Xiaojuan Qi. Parametric classification for generalized category discovery: A baseline study. In *Proceedings of the IEEE/CVF international conference on computer vision*, pages 16590–16600, 2023.
- [44] Yixin Fei, Zhongkai Zhao, Siwei Yang, and Bingchen Zhao. Xcon: Learning with experts for fine-grained category discovery. *arXiv preprint arXiv:2208.01898*, 2022.
- [45] Colin Troisemaine, Vincent Lemaire, Stéphane Gosselin, Alexandre Reiffers-Masson, Joachim Flocon-Cholet, and Sandrine Vatou. Novel class discovery: an introduction and key concepts. *arXiv preprint arXiv:2302.12028*, 2023.
- [46] Mathilde Caron, Ishan Misra, Julien Mairal, Priya Goyal, Piotr Bojanowski, and Armand Joulin. Unsupervised learning of visual features by contrasting cluster assignments. *Advances in neural information processing systems*, 33:9912–9924, 2020.
- [47] Marco Cuturi. Sinkhorn distances: Lightspeed computation of optimal transport. *Advances in neural information processing systems*, 26, 2013.
- [48] Alex Krizhevsky, Geoffrey Hinton, et al. Learning multiple layers of features from tiny images. 2009.
- [49] Catherine Wah, Steve Branson, Peter Welinder, Pietro Perona, and Serge Belongie. The caltech-ucsd birds-200-2011 dataset. 2011.
- [50] Harold W Kuhn. The hungarian method for the assignment problem. *Naval research logistics quarterly*, 2(1-2):83–97, 1955.

- [51] Tom Brown, Benjamin Mann, Nick Ryder, Melanie Subbiah, Jared D Kaplan, Prafulla Dhariwal, Arvind Neelakantan, Pranav Shyam, Girish Sastry, Amanda Askell, et al. Language models are few-shot learners. *Advances in neural information processing systems*, 33:1877–1901, 2020.
- [52] Tuomas Oikarinen and Tsui-Wei Weng. Clip-dissect: Automatic description of neuron representations in deep vision networks. *arXiv preprint arXiv:2204.10965*, 2022.
- [53] Ting Chen, Simon Kornblith, Mohammad Norouzi, and Geoffrey Hinton. A simple framework for contrastive learning of visual representations. In *International conference on machine learning*, pages 1597–1607. PmLR, 2020.
- [54] Yuki Markus Asano, Christian Rupprecht, and Andrea Vedaldi. Self-labelling via simultaneous clustering and representation learning. *arXiv preprint arXiv:1911.05371*, 2019.
- [55] Derek Weitzel, Ashton Graves, Sam Albin, Huijun Zhu, Frank Wuerthwein, Mahidhar Tatineni, Dmitry Mishin, Elham Khoda, Mohammad Sada, Larry Smarr, et al. The national research platform: Stretched, multi-tenant, scientific kubernetes cluster. In *Practice and Experience in Advanced Research Computing 2025: The Power of Collaboration*, pages 1–5, 2025.

A Concept Set Generation.

For all dataset we generated concepts following Oikarinen et al. [36], we generate initial concept sets using GPT [51] with three prompt types: (i) important features for recognizing each category, (ii) things commonly seen around each category, and (iii) superclasses. We apply filtering to remove: concepts longer than 30 characters, concepts too similar to category names (cosine similarity > 0.85), duplicate concepts (similarity > 0.9), concepts not present in training data, and concepts with poor projection accuracy (CLIP similarity < 0.35). The final concept counts are shown in Table 3.

CUB-200 dataset comes with expert annotated 312 concepts for all images and we generated 369 more concepts following the procedure described above and combined them together to have a total of 671 concepts. We have ran experiment on how our xNCD works with different concept sizes more details are in H.3

B Algorithm

B.1 Stage 1: Encoder Pretraining

- 1: **for** epoch = 1 to 200 **do**
- 2: **for** $(\mathbf{x}, y) \in \mathcal{D}^l$ **do**
- 3: $\mathbf{z} \leftarrow E_\theta(\mathbf{x})$
- 4: $\mathbf{p}^l \leftarrow \sigma(h(\mathbf{z})/\tau)$
- 5: $\mathcal{L} \leftarrow -\sum_c y_c \log p_c^l$
- 6: Update θ via SGD
- 7: **end for**
- 8: **end for**
- 9: Save pretrained encoder E_θ

B.2 Stage 2: Concept Layer Learning

- 1: Load pretrained encoder E_θ (frozen)
- 2: Extract features: $\mathbf{z}_i = E_\theta(\mathbf{x}_i)$ for all $\mathbf{x}_i \in \mathcal{D}^{\text{all}}$
- 3: Compute CLIP matrix: $P_{ij} = E_{\text{CLIP}}^{\text{img}}(\mathbf{x}_i) \cdot E_{\text{CLIP}}^{\text{txt}}(c_j)$ for all images
- 4: Initialize \mathbf{W}_c randomly
- 5: **for** training iterations with early stopping **do**
- 6: $\mathcal{L} \leftarrow \sum_{j=1}^K -\text{sim}(c_j, \mathbf{q}_j)$
- 7: Update \mathbf{W}_c via Adam optimizer
- 8: **end for**
- 9: Filter concepts: Keep only c_j where $\text{sim}(c_j, \mathbf{q}_j) \geq 0.35$
- 10: Update $K \leftarrow K - \Delta$ where Δ is number of filtered concepts
- 11: Save trained \mathbf{W}_c , concept normalization statistics, and final concept list

B.3 Stage 3: Concept-based Discovery

- 1: Load pretrained E_θ and trained \mathbf{W}_c
- 2: Initialize unlabeled heads $\{g_n\}$ and overclustering heads $\{o_n\}$
- 3: **for** epoch = 1 to 200 **do**
- 4: **for** batch $\mathcal{B} = \mathcal{B}^l \cup \mathcal{B}^u$ **do**
- 5: Generate views: $\{\mathbf{v}_1, \mathbf{v}_2\}$ for each $\mathbf{x} \in \mathcal{B}$
- 6: Extract concepts: $\hat{\mathbf{c}}_1 = \mathbf{W}_c E_\theta(\mathbf{v}_1)$, $\hat{\mathbf{c}}_2 = \mathbf{W}_c E_\theta(\mathbf{v}_2)$
- 7: Normalize: $\tilde{\mathbf{c}}_1 = (\hat{\mathbf{c}}_1 - \boldsymbol{\mu})/\boldsymbol{\sigma}$, $\tilde{\mathbf{c}}_2 = (\hat{\mathbf{c}}_2 - \boldsymbol{\mu})/\boldsymbol{\sigma}$
- 8: Compute logits: $\mathbf{l}_1 = [h(\tilde{\mathbf{c}}_1), g(\tilde{\mathbf{c}}_1)]$, $\mathbf{l}_2 = [h(\tilde{\mathbf{c}}_2), g(\tilde{\mathbf{c}}_2)]$
- 9: **For labeled samples:** $\mathbf{y}_1 = \mathbf{y}_2 = [\mathbf{y}^l, \mathbf{0}_{C_u}]$
- 10: **For unlabeled samples:** Generate $\hat{\mathbf{y}}_1, \hat{\mathbf{y}}_2$ via Sinkhorn-Knopp on $g(\tilde{\mathbf{c}})$
- 11: Compute loss: $\mathcal{L}_{\text{discovery}} = \mathbb{E}_{(\mathbf{v}_1, \mathbf{v}_2)} [\ell(\tilde{\mathbf{c}}_1, \hat{\mathbf{y}}_2) + \ell(\tilde{\mathbf{c}}_2, \hat{\mathbf{y}}_1)]$
- 12: Update parameters via SGD with momentum
- 13: **end for**
- 14: **end for**

C Similarity Function Details

C.1 Cubed Cosine Similarity for Concept Alignment

In Stage 2, we align learned concept activations with CLIP’s vision-language similarity priors. We use a cubed cosine similarity function (Equation (4)):

$$\text{sim}(\mathbf{q}_j, \mathbf{P}_{:,j}) = \frac{\bar{\mathbf{q}}_j^3 \cdot \bar{\mathbf{P}}_{:,j}^3}{\|\bar{\mathbf{q}}_j^3\|_2 \|\bar{\mathbf{P}}_{:,j}^3\|_2}$$

where $\bar{\mathbf{v}}$ denotes mean-centered and standardized \mathbf{v} , and the cube is applied element-wise.

C.2 Motivation

Standard cosine similarity weights all samples equally when measuring correlation between activation patterns. However, for concept alignment in novel category discovery, this uniform weighting is suboptimal for two reasons:

Sparse concept presence. Most concepts are present in only a small fraction of images. For example, a concept like “striped” may be strongly present in a small subset of images while being absent or ambiguous in the remainder. Standard cosine similarity dilutes the signal from these informative samples with noise from the majority.

Gradient signal concentration. During optimization, we want gradients to flow primarily from samples where the concept is clearly present or clearly absent, not from ambiguous cases where CLIP’s assessment may be unreliable.

Polynomial amplification addresses both issues by emphasizing extreme values. For a standardized activation $\bar{v}_i \in [-3, 3]$ (approximately), the cubic power preserves sign while amplifying magnitude for $|\bar{v}_i| > 1$, effectively reweighting samples so high-activation images contribute disproportionately to the similarity score [52, 36].

Concepts with similarity below $\delta_{\text{align}} = 0.35$ are filtered out, ensuring that retained concepts are faithfully represented in the concept bottleneck layer. Table 5 (Appendix H) shows that this approach achieves average CLIP similarity between 0.371–0.487 across datasets, with concept retention rates of 65–92%, indicating effective concept learning in our NCD setting.

D Multi-view Self-labeling and Pseudo-label Generation

In this section, we describe how multi-view self-labeling is used to generate pseudo-labels for our unified objective. This approach, originally developed for self-supervised and semi-supervised learning [46, 53], enables effective knowledge transfer from labeled to unlabeled data.

D.1 Multi-view Generation

Given an image \mathbf{x} , we generate two augmented views \mathbf{v}_1 and \mathbf{v}_2 by applying random transformations consisting of random cropping, color jittering, and horizontal flipping. These augmentations, which have proven effective in contrastive learning [53], encourage the model to learn transformation-invariant representations.

For labeled samples $(\mathbf{x}, y^l) \in \mathcal{D}^l$, both views are associated with the same ground-truth label, padded with zeros for the novel categories:

$$\mathbf{y}_1 = \mathbf{y}_2 = [y^l, \mathbf{0}_{C_u}]. \tag{16}$$

For unlabeled samples $\mathbf{x} \in \mathcal{D}^u$, we use the *swapped prediction* task [46]: the pseudo-label computed from one view serves as the target for the other view:

$$\mathbf{y}_1 = [\mathbf{0}_{C_l}, \hat{\mathbf{y}}_2], \quad \mathbf{y}_2 = [\mathbf{0}_{C_l}, \hat{\mathbf{y}}_1]. \tag{17}$$

This formulation encourages the model to output consistent predictions for different augmentations of the same image. When evaluating each term in the loss, we apply a stop-gradient for the pseudo-label, i.e., the gradient flows only through the prediction branch.

D.2 Pseudo-label Generation via Optimal Transport

A naïve approach to generate pseudo-labels would be to directly use the softmax outputs of $g(\tilde{\mathbf{c}})$, setting $\hat{\mathbf{y}}_2 = \sigma(g(\tilde{\mathbf{c}}_1)/\tau)$. However, as observed in Asano et al. [54], this may lead to degenerate solutions where the model always predicts the same cluster for any input—in this case, the prediction and pseudo-label become identical and no learning occurs.

To prevent such collapse, we compute pseudo-labels using the Sinkhorn-Knopp algorithm [47], which adds an entropy regularizer that encourages uniform partition of pseudo-labels across all clusters. For a mini-batch containing B^u unlabeled samples, let $\mathbf{L} = [\mathbf{l}_1, \dots, \mathbf{l}_{B^u}] \in \mathbb{R}^{C_u \times B^u}$ be the matrix whose columns are the concept-space logits computed by $g(\tilde{\mathbf{c}})$. The pseudo-label matrix $\hat{\mathbf{Y}} = [\hat{\mathbf{y}}_1, \dots, \hat{\mathbf{y}}_{B^u}]^\top \in \mathbb{R}^{C_u \times B^u}$ is obtained by solving:

$$\hat{\mathbf{Y}} = \arg \max_{\mathbf{Y} \in \Gamma} \text{Tr}(\mathbf{Y}\mathbf{L}^\top) + \epsilon \text{H}(\mathbf{Y}), \quad (18)$$

where $\epsilon > 0$ is a hyperparameter, $\text{H}(\mathbf{Y}) = -\sum_{ij} Y_{ij} \log Y_{ij}$ is the entropy function used to “scatter” the pseudo-labels, and Γ is the transportation polytope defined as:

$$\Gamma = \left\{ \mathbf{Y} \in \mathbb{R}_+^{C_u \times B^u} \mid \mathbf{Y}\mathbf{1}_{B^u} = \frac{1}{C_u} \mathbf{1}_{C_u}, \mathbf{Y}^\top \mathbf{1}_{C_u} = \frac{1}{B^u} \mathbf{1}_{B^u} \right\}. \quad (19)$$

These constraints enforce that, on average, each cluster is selected B^u/C_u times per batch, preventing any single cluster from dominating. Following Caron et al. [46], we use 3 Sinkhorn iterations with $\epsilon = 0.05$. The resulting pseudo-labels $\hat{\mathbf{y}}_j \in [0, 1]^{C_u}$ are soft assignments; we found that using soft pseudo-labels yields better performance than discretizing them.

D.3 Concept-Space Pseudo-labels: The Key Difference

The critical distinction between xNCD and standard NCD methods lies in *where* pseudo-labels are computed. In prior work such as UNO [26], pseudo-labels are generated from opaque feature representations cluster assignments reflect arbitrary similarities in high-dimensional feature space with no semantic meaning.

In xNCD, pseudo-labels are computed from concept-space logits $g(\tilde{\mathbf{c}})$, where $\tilde{\mathbf{c}} \in \mathbb{R}^K$ represents interpretable concept activations. This design choice has two important consequences:

1. **Interpretable clustering:** Samples are grouped together because they share similar *concept activations*, not because of opaque feature correlations. A cluster of dogs emerges because its members all activate “four-legged,” “furry,” and “mammal” concepts.
2. **Semantic consistency:** The Sinkhorn-Knopp constraints operate in concept space, encouraging each discovered cluster to have a coherent concept profile rather than arbitrary feature statistics.

This is the architectural modification that enables xNCD to provide human-understandable explanations for discovered categories while maintaining competitive clustering performance.

E Formal Definitions of Explanations

E.1 Interpretable Cluster Characterization

A key advantage of xNCD is that discovered clusters admit human-understandable descriptions through their concept activation profiles.

E.1.1 Cluster-Level Signatures

After discovery, each novel category $i \in \{1, \dots, C_u\}$ is characterized by its mean concept activation vector. Let $S_i = \{\mathbf{x} \in \mathcal{D}^u \mid \hat{y}(\mathbf{x}) = C_i + i\}$ denote samples assigned to cluster i . The cluster’s concept profile is:

$$\bar{\mathbf{c}}^{(i)} = \frac{1}{|S_i|} \sum_{\mathbf{x} \in S_i} \tilde{\mathbf{c}}(\mathbf{x}) \in \mathbb{R}^K. \quad (20)$$

The top- r activated concepts provide a semantic signature:

$$\text{Signature}(i) = \text{Top}_r(\bar{\mathbf{c}}^{(i)}), \quad (21)$$

where Top_r returns indices of the r concepts with highest mean activation. In our experiments, we use $r = 10$ to provide concise yet informative cluster characterizations.

E.1.2 Instance-Level Explanations

For a test image \mathbf{x} predicted as novel category i , we explain the prediction by identifying which signature concepts are strongly activated:

$$\text{Explanation}(\mathbf{x}, i) = \{c_j \mid \tilde{c}_j(\mathbf{x}) > \delta_{\text{explain}}, j \in \text{Signature}(i)\}, \quad (22)$$

where δ_{explain} is an activation threshold. In our experiments, we use $\delta_{\text{explain}} = 0$ (i.e., include all positively activated signature concepts).

This enables explanations such as: “*This image belongs to novel category 3 because it strongly activates concepts {four-legged, fur, tail} which characterize this cluster.*” Such explanations allow domain experts to validate whether discovered categories are semantically meaningful and to identify potential failure modes.

F Implementation Details

During pre-training stage 1, we pretrain the encoder for 200 epochs on labeled data using SGD with momentum 0.9 (lr=0.1, cosine annealing, weight decay 10^{-4}). Temperature $\tau = 0.1$ for all softmax layers. In Stage 2, we train the concept projection W_c for 1000 iterations using Adam optimizer (lr= 10^{-3}) with early stopping (patience=5 validation checks). We use an 80/20 train/validation split. The projection batch size is 50,000 samples. Concepts with CLIP similarity below $\delta_{\text{align}} = 0.35$ are filtered out.

In the discovery phase, we train for 200 epochs using SGD with momentum 0.9 (base lr=0.4, weight decay 1.5×10^{-4}). We use 5 clustering heads with overclustering factor 3. The Sinkhorn-Knopp algorithm uses 3 iterations with $\epsilon = 0.05$. Concept activations are normalized using statistics computed in Stage 2: $\tilde{c} = (W_c z - \mu) / \sigma$, where $\mu, \sigma \in \mathbb{R}^K$ are per-concept mean and standard deviation.

G Dataset Statistics

Table 3: Statistics of the datasets and splits used in our novel category discovery benchmark. Each dataset is split into disjoint labeled (known) and unlabeled (novel) category sets.

Dataset	Labeled		Unlabeled		K
	Images	categories	Images	categories	
CIFAR-10	25K	5	25K	5	143
CIFAR-100	40K	80	10K	20	892
CUB-200	8.5K	170	1.4K	30	671

H Ablation Study

H.1 Clustering Quality Metrics

We evaluate clustering quality using NMI and ARI (Table 4). xNCD achieves strong clustering coherence, with NMI of 86.34% and ARI of 85.11% on CIFAR-10 under task-aware evaluation, indicating that discovered clusters are semantically meaningful.

Table 4: Clustering quality metrics on novel categories.

Dataset	Task-Aware		Task-Agnostic	
	NMI	ARI	NMI	ARI
CIFAR-10	86.34 \pm 0.3	85.11 \pm 0.4	83.22 \pm 0.4	83.21 \pm 0.5
CIFAR-100	79.00 \pm 0.5	70.39 \pm 0.6	76.63 \pm 0.6	65.36 \pm 0.7
CUB-200	63.57 \pm 0.8	33.39 \pm 1.0	65.73 \pm 0.9	34.31 \pm 1.1

H.2 Concept Set Statistics.

Table 5 summarizes concept filtering across datasets. Initial concepts are generated via GPT-3, then pre-filtered to remove duplicates and category-similar concepts. After Stage 2 training, we apply a second filtering step: concepts with learned CLIP similarity below threshold $\delta_{\text{align}} = 0.35$ are removed, as they indicate poor alignment between the projection layer and CLIP’s semantic understanding. This ensures all retained concepts are faithfully represented in the concept bottleneck layer.

Table 5: Concept set statistics. *Generated*: after initial filtering (Appendix A). *Final*: after Stage 2 CLIP similarity filtering ($\delta_{\text{align}} = 0.35$). *Avg. Sim.*: average CLIP similarity of retained concepts.

Dataset	Generated	Final	Avg. Sim.
CIFAR-10	143	131	0.487
CIFAR-100	892	422	0.371
CUB-200	671	453	0.402

H.3 Effect of Concept Vocabulary Size

Table 6 examines how concept vocabulary size affects discovery on CUB-200. We evaluate expert-annotated attributes (312 concepts), GPT-generated descriptions (369 concepts), and their combination (671 concepts).

Results demonstrate that larger vocabularies improve performance: the combined set achieves 67.88%, outperforming smaller vocabularies by approximately 5%. This suggests that richer concept spaces provide more discriminative dimensions for distinguishing fine-grained novel categories. Additionally, the comparable performance between expert and GPT concepts indicates that concept diversity may be as important as domain-specific quality for novel category discovery.

Table 6: Ablation study on concept source for CUB-200 (170+30 split). Expert concepts are domain-specific bird attributes, GPT concepts are LLM-generated descriptions.

Concept Source	# Concepts	Accuracy (%)
Combined	671	67.88
GPT-generated	369	63.12
Expert-annotated	312	64.48

I Discussion

Summary of Findings. Our experiments demonstrate that xNCD successfully bridges interpretability and novel category discovery. On standard benchmarks, xNCD achieves clustering accuracy within 1-3% of state-of-the-art methods (92.63% vs. UNO’s 93.4% on CIFAR-10) while being the only method to provide human-understandable explanations for discovered categories. Notably, on CIFAR-100 under task-agnostic evaluation, xNCD outperforms UNO (76.45% vs. 73.2%), suggesting that concept-based representations may offer advantages for distinguishing between known and novel categories.

The Accuracy-Interpretability Trade-off. Our results reveal a nuanced trade-off between clustering performance and interpretability. Removing the concept bottleneck layer entirely (operating in raw

feature space) yields a 1-2% accuracy improvement, confirming that the concept layer introduces some information bottleneck. However, this cost is modest and is offset by the substantial interpretability benefits: discovered clusters can be characterized through concept profiles, enabling domain expert validation and model debugging.

Limitations. Our approach inherits limitations from both concept bottleneck models and novel category discovery. First, the concept vocabulary must be either generated (via LLMs) or annotated by domain experts, and our dependency on CLIP may miss domain-specific attributes—particularly problematic for specialized domains (e.g., medical imaging) where CLIP lacks relevant training data. Second, like most NCD methods, we assume the number of novel categories C_u is known a priori; real-world open-world scenarios may contain substantially more novel categories than our experimental settings. Finally, while our unified objective eliminates self-supervised pretraining, performance still depends on semantic similarity between labeled and unlabeled categories for effective knowledge transfer.

Broader Impact. xNCD enables interpretable open-world learning, with potential applications in scientific discovery domains where understanding *why* categories emerge is as important as discovering them. In biodiversity monitoring, ecologists could validate whether discovered species groupings reflect meaningful taxonomic distinctions. In drug discovery, novel compound clusters could be characterized through interpretable molecular properties. We do not foresee negative societal consequences specific to this work.

J Visualization

J.1 Cluster-wise Explanation

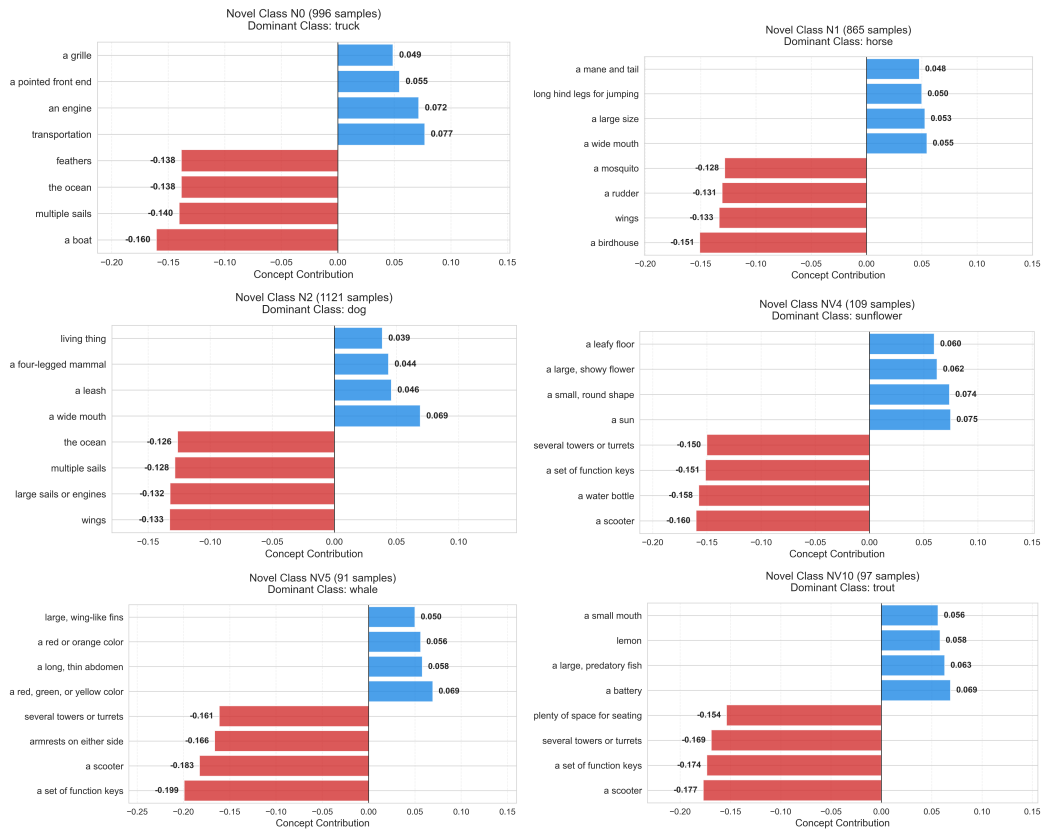


Figure 6: Additional cluster-level concept profiles for discovered novel categories

J.2 Instance level Explanation

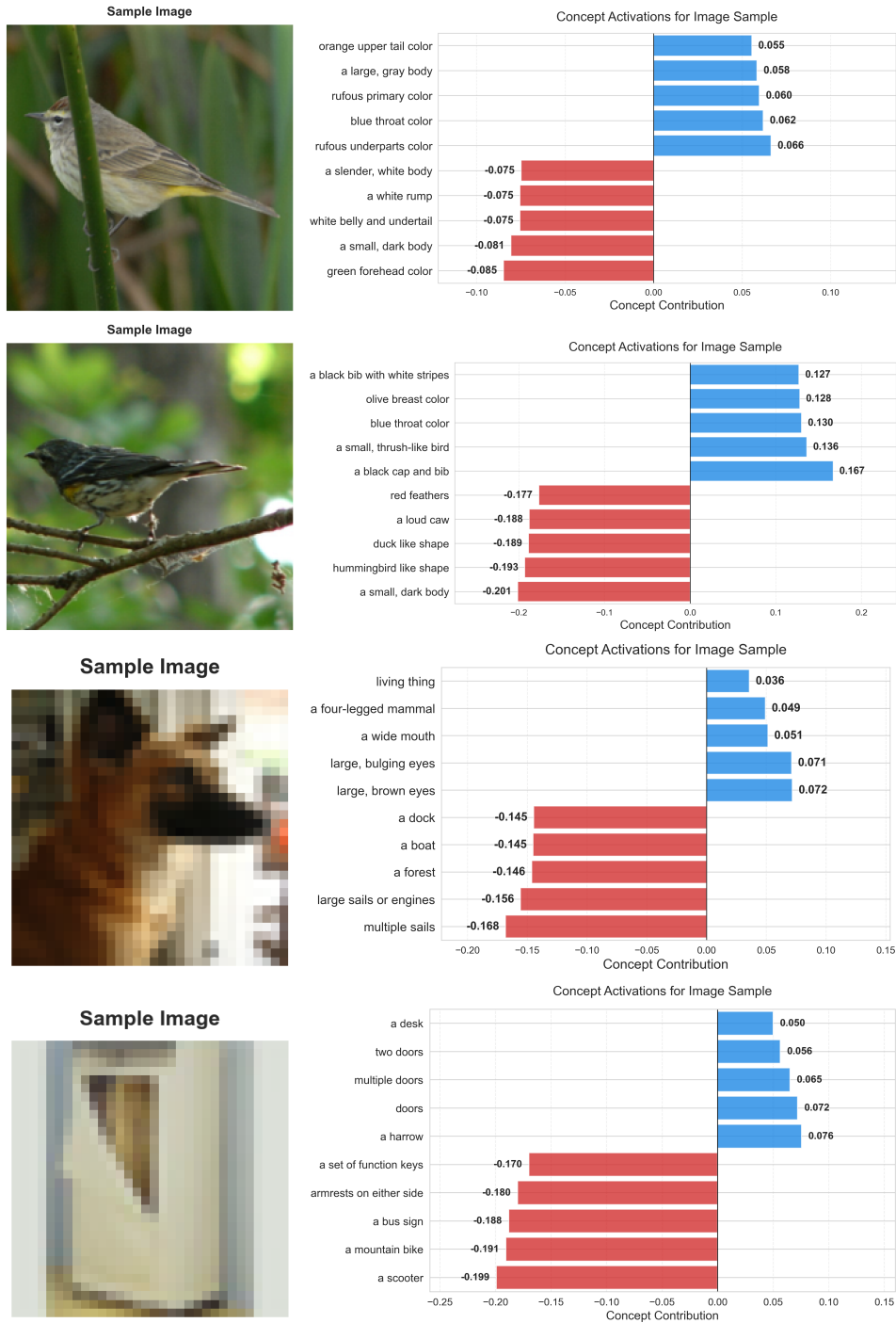


Figure 7: Additional instance-level concept explanations for samples from CUB-200, CIFAR-10, and CIFAR-100.

K Experiments Computing Resources

All experiments were performed on NRP Nautilus HPC [55]. Training and evaluation used a single GPU for CIFAR10/100 and two GPU for CUB-200 dataset per experiment. Node specifications are provided in Table 7.

Table 7: Hardware configuration for experiments

Component	Configuration
CPUs	Dual 12-core SkyLake 5000 series
GPUs	Nvidia RTX A6000 64GB
RAM	32GB
SSD	240GB

NeurIPS Paper Checklist

1. Claims

Question: Do the main claims made in the abstract and introduction accurately reflect the paper’s contributions and scope?

Answer: [Yes]

Justification: The abstract and introduction accurately reflect the paper’s contributions. The claims cover (i) concept-space NCD framework, (ii) competitive empirical performance on CIFAR-10/100 and CUB-200, and (iii) theoretical hypothesis-space restriction via concept bottleneck, all of which are supported by experiments.

2. Limitations

Question: Does the paper discuss the limitations of the work performed by the authors?

Answer: [Yes]

Justification: We have discussed the limitations of our methodology in Appendix I, where we reflect on potential areas for improvement and further exploration

3. Theory assumptions and proofs

Question: For each theoretical result, does the paper provide the full set of assumptions and a complete (and correct) proof?

Answer: [Yes]

Justification: Proposition 4.1 states assumptions explicitly (linearity of concept map, $K < \min\{C, dz\}$) and provides a complete proof in the main paper. The semantic anchoring constraint beyond rank restriction is discussed following the proposition.

4. Experimental result reproducibility

Question: Does the paper fully disclose all the information needed to reproduce the main experimental results of the paper to the extent that it affects the main claims and/or conclusions of the paper (regardless of whether the code and data are provided or not)?

Answer: [Yes]

Justification: All information needed to reproduce the main results is provided in the paper, independent of the supplemental code. Full implementation details are provided in Appendix F, including optimizer settings, learning rates, batch sizes, number of epochs, Sinkhorn hyperparameters, and concept filtering thresholds. Dataset splits are specified in Appendix G. Algorithms for all three stages are provided in Appendix B.

5. Open access to data and code

Question: Does the paper provide open access to the data and code, with sufficient instructions to faithfully reproduce the main experimental results, as described in supplemental material?

Answer: [Yes]

Justification: Anonymized code is provided as supplemental material with instructions to reproduce the experimental results. The datasets used (CIFAR-10, CIFAR-100, and CUB-200) are publicly available.

6. Experimental setting/details

Question: Does the paper specify all the training and test details (e.g., data splits, hyperparameters, how they were chosen, type of optimizer) necessary to understand the results?

Answer: [Yes]

Justification: Training and evaluation details are provided in Section 5 and Appendix F, including backbone architecture, optimizer, learning rate schedule, temperature, number of clustering heads, Sinkhorn iterations, and concept alignment threshold. Dataset splits are described in Appendix G.

7. Experiment statistical significance

Question: Does the paper report error bars suitably and correctly defined or other appropriate information about the statistical significance of the experiments?

Answer: [Yes]

Justification: All main results in Table 1 and Table 4 report mean \pm standard deviation across 3 runs, capturing variability due to random initialization. Error bars are reported consistently across all datasets and evaluation protocols.

8. Experiments compute resources

Question: For each experiment, does the paper provide sufficient information on the computer resources (type of compute workers, memory, time of execution) needed to reproduce the experiments?

Answer: [Yes]

Justification: In the appendix K section of this paper, we have clearly outlined the hardware configuration used to run the experiments for the proposed methods.

9. Code of ethics

Question: Does the research conducted in the paper conform, in every respect, with the NeurIPS Code of Ethics <https://neurips.cc/public/EthicsGuidelines>?

Answer: [Yes]

Justification: The research uses publicly available datasets and does not involve human subjects, sensitive data collection, or potential for direct harm. The work has been conducted in accordance with the NeurIPS Code of Ethics.

10. Broader impacts

Question: Does the paper discuss both potential positive societal impacts and negative societal impacts of the work performed?

Answer: [Yes]

Justification: Broader impact is discussed in Appendix I, covering positive applications in scientific discovery, biodiversity monitoring, and drug discovery. The authors do not foresee specific negative societal consequences from this work.

11. Safeguards

Question: Does the paper describe safeguards that have been put in place for responsible release of data or models that have a high risk for misuse (e.g., pre-trained language models, image generators, or scraped datasets)?

Answer: [N/A]

Justification: The method performs category discovery on standard vision benchmarks and poses no identified risks requiring safeguards. As such, it does not involve the release of data or models that carry a high risk of misuse, and therefore, no specific safeguards are required.

12. Licenses for existing assets

Question: Are the creators or original owners of assets (e.g., code, data, models), used in the paper, properly credited and are the license and terms of use explicitly mentioned and properly respected?

Answer: [Yes]

Justification: The datasets used in this paper (CIFAR-10, CIFAR-100, and CUB-200) are publicly available. We have ensured that the terms of use for these datasets are respected, and the corresponding citations are included in the paper.

13. New assets

Question: Are new assets introduced in the paper well documented and is the documentation provided alongside the assets?

Answer: [Yes]

Justification: Our work does not create new assets such as datasets, However Anonymized code is submitted as supplemental material.

14. Crowdsourcing and research with human subjects

Question: For crowdsourcing experiments and research with human subjects, does the paper include the full text of instructions given to participants and screenshots, if applicable, as well as details about compensation (if any)?

Answer: [N/A]

Justification: This paper does not involve crowdsourcing or research with human subjects. All experiments are conducted on existing publicly available image classification benchmarking dataset.

15. Institutional review board (IRB) approvals or equivalent for research with human subjects

Question: Does the paper describe potential risks incurred by study participants, whether such risks were disclosed to the subjects, and whether Institutional Review Board (IRB) approvals (or an equivalent approval/review based on the requirements of your country or institution) were obtained?

Answer: [N/A]

Justification: Our Work does not involve research with human subjects, and therefore, IRB approval or equivalent was not required.

16. Declaration of LLM usage

Question: Does the paper describe the usage of LLMs if it is an important, original, or non-standard component of the core methods in this research? Note that if the LLM is used only for writing, editing, or formatting purposes and does *not* impact the core methodology, scientific rigor, or originality of the research, declaration is not required.

Answer: [N/A]

Justification: LLMs are not an important, original, or non-standard component of the proposed method. Concept set generation follows the established pipeline of Oikarinen et al. [36], which uses GPT API as a standard component of prior work and not a novel contribution of this paper. Any additional LLM usage was limited to writing assistance (grammar and editing) and did not impact the scientific rigor or originality of the research.